

Ceruloplasmin/Hephaestin Knockout Mice Model Morphologic and Molecular Features of AMD

Majda Hadziabmetovic,¹ Tzvetze Dentchev,¹ Ying Song,¹ Nadine Haddad,¹ Xining He,¹ Paul Hahn,¹ Domenico Pratico,² Rong Wen,³ Z. Leah Harris,⁴ John D. Lambris,⁵ John Beard,⁶ and Joshua L. Dunaief¹

PURPOSE. Iron is an essential element in human metabolism but also is a potent generator of oxidative damage with levels that increase with age. Several studies suggest that iron accumulation may be a factor in age-related macular degeneration (AMD). In prior studies, both iron overload and features of AMD were identified in mice deficient in the ferroxidase ceruloplasmin (Cp) and its homologue hephaestin (Heph) (double knockout, DKO). In this study, the location and timing of iron accumulation, the rate and reproducibility of retinal degeneration, and the roles of oxidative stress and complement activation were determined.

METHODS. Morphologic analysis and histochemical iron detection by Perls' staining was performed on retina sections from DKO and control mice. Immunofluorescence and immunohistochemistry were performed with antibodies detecting activated complement factor C3, transferrin receptor, L-ferritin, and macrophages. Tissue iron levels were measured by atomic absorption spectrophotometry. Isoprostone F2 α -VI, a specific marker of oxidative stress, was quantified in the tissue by gas chromatography/mass spectrometry.

RESULTS. DKOs exhibited highly reproducible age-dependent iron overload, which plateaued at 6 months of age, with subsequent progressive retinal degeneration continuing to at least 12 months. The degeneration shared some features of AMD, including RPE hypertrophy and hyperplasia, photoreceptor degeneration, subretinal neovascularization, RPE lipofuscin accumulation, oxidative stress, and complement activation.

CONCLUSIONS. DKOs have age-dependent iron accumulation followed by retinal degeneration modeling some of the morpho-

logic and molecular features of AMD. Therefore, these mice are a good platform on which to test therapeutic agents for AMD, such as antioxidants, iron chelators, and antiangiogenic agents. (*Invest Ophthalmol Vis Sci.* 2008;49:2728-2736) DOI:10.1167/iov.07-1472

Iron is a trace element that functions as a component of many proteins and enzymes, including oxygen-carrying proteins hemoglobin and myoglobin, cytochromes, and other enzymes that are involved in oxidation or reduction. Although iron is an essential metabolic component, it is also a potent generator of damaging free radicals that can cause oxidative stress. Regulation of ferrous iron levels is critical for meeting physiologic demand while preventing the toxicity associated with iron overload.¹

Iron absorption in the intestine generally exceeds iron elimination from the body, leading to an age-dependent increase in iron levels in many tissues, including the retina.² With aging, the levels of serum ferritin, a measure of total body stores, increase.³ The age-associated increase in iron may contribute to age-related degenerative diseases.

Iron is absorbed in the intestine and then delivered to the target tissues by the plasma iron transport protein transferrin (Tf). Transferrin-iron complexes bind to transferrin receptor (TfR)-I on the cell membrane and undergo internalization by receptor-mediated endocytosis.⁴ Iron is then used for cellular metabolism, and excess iron is stored in the storage protein ferritin. Intracellular levels of ferritin are posttranscriptionally controlled by the iron regulatory proteins IRP-1 and -2. Increased iron leads to increased cytosolic ferritin mRNA translation, which in turn increases ferritin levels.⁵

Iron export from the cells is facilitated by ceruloplasmin (Cp), a multicopper ferroxidase. Cp oxidizes ferrous to ferric iron, the only form that can be taken up by the serum transport protein transferrin.^{6,7} Hephaestin (Heph) is another multicopper ferroxidase with 50% identity to Cp that also facilitates iron export.⁸ Heph is naturally mutated in sex-linked anemia (*Sla*) mice.⁹

Accumulation of body iron stores may be important in both aging and age-related diseases, including retinal diseases.¹⁰ Patients with the disease aceruloplasminemia, a hereditary deficiency in Cp, have defective export of iron from some tissues including the retina,^{11,12} resulting in macular degeneration beginning in the fourth decade.¹³ Previously, we have found that AMD-affected maculas have significantly increased total iron concentration,¹⁴ compared with age-matched controls, suggesting that iron accumulation may play a role in this disease.

Age-related macular degeneration (AMD) is the most common cause of vision loss in the United States and other developed nations among people 65 years of age and older.¹⁵ Although the pathogenesis of AMD is incompletely understood, evidence suggests that oxidative stress and inflammation may mediate or exacerbate macular degeneration.¹ Because iron overload has been implicated in age-related neurodegenerative diseases such as Alzheimer's and Parkinson's disease,¹⁶ and also in the macular degeneration occurring in patients with the rare autosomal recessive disease aceruloplasminemia,¹ we investigated iron's contribution to AMD.

From the ¹F. M. Kirby Center for Molecular Ophthalmology, Scheie Eye Institute, and the ²Department of Pathology and Laboratory Medicine, University of Pennsylvania, Philadelphia, Pennsylvania; the ³Department of Pharmacology, Temple University, Philadelphia, Pennsylvania; the ⁴Department of Ophthalmology, Bascom Palmer Eye Institute, University of Miami, Miami, Florida; the ⁵Department of Pediatric Anesthesia and Critical Care, The Johns Hopkins School of Medicine, Baltimore, Maryland; and the ⁶Department of Nutrition, College of Health and Human Development, Pennsylvania State University, University Park, Pennsylvania.

Supported by an unrestricted grant and a William and Mary Greeve Scholar Award (JLD) from Research to Prevent Blindness; National Eye Institute Grant EY015240; the Macula Vision Research Foundation, the Jahnigen Career Development Award (JLD) from the American Geriatrics Society; the F. M. Kirby Foundation; the International Retina Research Foundation; and the Paul and Evanina Bell MacKall Foundation Trust.

Submitted for publication November 15, 2007; revised January 23 and February 6, 2008; accepted April 16, 2008.

Disclosure: **M. Hadziabmetovic**, None; **T. Dentchev**, None; **Y. Song**, None; **N. Haddad**, None; **X. He**, None; **P. Hahn**, None; **D. Pratico**, None; **R. Wen**, None; **Z.L. Harris**, None; **J.D. Lambris**, None; **J. Beard**, None; **J.L. Dunaief**, None

The publication costs of this article were defrayed in part by page charge payment. This article must therefore be marked "advertisement" in accordance with 18 U.S.C. §1734 solely to indicate this fact.

Corresponding author: Joshua L. Dunaief, 305 Stellar-Chance Labs, 422 Curie Boulevard, Philadelphia, PA, 19104; jdunaief@mail.med.upenn.edu.

To test the hypothesis that deficiency in both Cp and Heph would induce retinal iron overload and neurodegeneration, we generated mice harboring both the Cp knockout allele and a Heph mutation from *Sla* mice and refer to them herein as double knockout (DKO).⁸ Previously, we found that combined deficiency in Cp and Heph results in retinal iron accumulation with increases in several forms of the iron storage protein ferritin, and ultimately, retinal degeneration.⁸ This degeneration shares many features with AMD, including photoreceptor and RPE death, sub-RPE deposits, and subretinal neovascularization. The viability of the DKO mice is limited by an age-dependent movement disorder, and our initial report on these mice was limited in number and age (9 months and younger). We now report details of retinal degeneration in a study of a larger number of DKO mice, including some that lived to 13 months of age—to date, the longest-lived DKO mice. In the present study, we performed a detailed analysis of the rate of iron accumulation and found that iron levels in the retina and RPE/choroid continued to increase until 6 months of age, followed by progressive retinal degeneration. Further, we provide evidence that oxidative stress and activation of the complement cascade may be involved in the retinal degeneration. Finally, we report iron accumulation and elevated ferritin in the DKO ciliary body.

MATERIALS AND METHODS

Animals

C57BL/6 wild-type mice, C57BL/6 mice with a targeted mutation in the Cp gene (Cp^{-/-}), and naturally occurring *Sla* mutation in the Heph gene (Heph^{-/-} or Heph^{-Y}) were used.⁸ All procedures were approved by the Institutional Animal Care and Use Committee of the University of Pennsylvania and complied with the ARVO Statement for the Use of Animals in Ophthalmic and Vision Research.

The eyes were enucleated immediately after the death of the and were either fixed overnight in 2% paraformaldehyde (PFA) and 2% glutaraldehyde for histochemical iron detection and morphologic analysis or were lightly fixed for 2 hours in 4% paraformaldehyde (PFA) for immunohistochemistry. For morphology, $n = 6$ for mice younger than 6 months, $n = 15$ for mice 6 to 9 months, and $n = 4$ for mice 12 to 13 months old.

Quantitative Iron Detection

After enucleation, the eyes from wild-type and DKO mice were fixed in 4% PFA for several days. Eyecups were made by removing the anterior segment. The ciliary body was removed with a curved scalpel blade, and the neurosensory retina was then detached from the underlying RPE/choroid tissue, taking care to minimize disruption of the RPE. Samples of the retina and RPE/choroids (with sclera) were placed in separate tubes, and dried for 5 days at room temperature.

Iron in these tissues was measured by graphite furnace atomic absorption spectrophotometry (model 5100 AA; Perkin Elmer, Boston, MA), according to standard methods.^{8,17}

Isoprostane Quantification

For biochemical analysis of isoprostane F2 α -VI levels, a chemically stable, specific marker of oxidative stress, mice were killed, and the retinas were isolated immediately and collected on dry ice. The retinas were homogenized, and total lipids were extracted as previously published.¹⁸ After mass spectrometry, quantification was performed by using the peak area ratio.^{19,20}

Statistical Analysis

The mean \pm SE of iron levels in retina and RPE/choroid were calculated for wild-type and knockout groups. The means between wild-type and knockout mice of the same age were compared using the two group *t*-test. $P < 0.05$ was considered to be statistically significant. All statistical analysis was performed with commercial software (SAS, ver. 9.1; SAS Institute, Inc., Cary, NC).

Histochemical Iron Detection by Perls' Staining and Morphology Analysis

Fixed globes were rinsed in PBS and the eyecups were prepared by removing the anterior segment. The tissues were dehydrated through a graded series of ethanol and infiltrated over night in 1.25% benzoyl peroxide in embedding solution (JB4 Solution A; Polysciences, Inc., Warrington, PA). The next day, the eyecups were oriented and embedded in plastic (JB-4; Polysciences, Inc.). Plastic sections 3 μ m thick were Perls' stained for histochemical iron detection by incubation in 5% potassium ferrocyanide (J. T. Baker, Phillipsburg, NJ) in 5% aqueous hydrochloric acid (Sigma-Aldrich, St. Louis, MO) for 30 minutes at room temperature yielding a Prussian blue reaction product. Sensitivity for iron detection was enhanced by subsequent incubation of tissue in purple peroxidase substrate for 25 minutes at room temperature (VIP; Vector Laboratories, Inc., Burlingame, CA). For standard histology toluidine blue staining was performed by incubation of the sections in 1% toluidine blue O and 1% sodium tetraborate decahydrate (Sigma-Aldrich) for 5 seconds. Stained sections were observed and photographed with a microscope (model TE-300; Nikon, Tokyo, Japan).

Immunofluorescence and Immunohistochemistry

The fixed globes were rinsed in PBS and the eyecups were dissected. The eyecups were cryoprotected overnight in 30% sucrose and embedded in optimal cutting temperature compound (OCT; Tissue-Tek; Sakura Finetek, Torrance, CA). Immunofluorescence was performed on cryosections 10 μ m thick, as previously published.²¹ Primary antibodies used were rat anti-mouse C3b/iC3b/C3c, (1:10 dilution; the generous gift of John Lambris, University of Pennsylvania, Philadelphia), which detects the cleavage products of complement factor C3; rabbit anti-human TFR antibodies (1:100; Zymed Laboratories, Inc., San Francisco, CA); rabbit anti-light ferritin (F17) antibodies (1:2500; the kind gift of Paolo Santambrogio and Paolo Arosio, IRCCS, Milan, Italy), rat anti-mouse F4/80 (1:50 dilution; Serotec, Martinsried, Germany). Primary antibody reactivity was detected with fluorophore-labeled secondary antibodies (Jackson ImmunoResearch Laboratories, Inc., West Grove, PA). The control sections were treated identically but with omission of the primary antibody. The sections were analyzed by fluorescence microscopy with identical exposure parameters. Immunohistochemistry was performed according to the manufacturer's instructions (Vectastain ABC-AP Kit; Vector Laboratories, Inc.). The primary antibodies were rat anti-mouse CD11b (1:100 dilution; BD Biosciences, San Jose, CA). Chromogenic visualization was performed with a biotinylated polyclonal anti-rat IgG, together with the BCIP/NBT detection system (Vector Laboratories, Inc.) for 15 minutes. The control sections were treated identically but with omission of the primary antibody. The sections were analyzed by bright-field microscopy.

Fluorescent Blood Vessel Labeling

Blood vessels were directly labeled with a solution containing a fluorescent carbocyanine dye DiI (1,1'-dioctadecyl-3,3',3'-tetramethylindocarbocyanine perchlorate; Sigma-Aldrich), as described by Zhao et al.²² The mice were killed and perfused with PBS (4–5 mL), followed by a solution containing 160 mM DiI (4–5 mL). They were subsequently perfused with 4% paraformaldehyde (20 mL in 0.1 M phosphate buffer; pH 7.4), and the eyes were harvested and the anterior segments removed. The eyecups were examined with an epifluorescence microscope (Stemi SV11; Carl Zeiss Meditec, Dublin, CA) and imaged with a digital camera (Axiocam; Carl Zeiss Meditec.).

RESULTS

Perls' Staining for Iron in the Retina and Ciliary Body in Wild-Type and Cp^{-/-}Heph^{-Y} (DKO) Mice

As previously published,⁸ at the age of 5 to 6 months DKO retinas had increased iron, with the highest levels in present in

the RPE. In this study, we also Perls' stained the ciliary body. Because iron tends to accumulate in the retina with age,¹⁰ we tested whether 16-month-old wild-type mice had any iron accumulation in the retina or ciliary body. Neither a 16-month-old (Fig. 1A) nor 7-month-old wild-type retina (not shown) had any Perls' label in the ciliary body or retina. In contrast, the 7-month-old DKO ciliary body had a strong granular Perls' stain (Fig. 1B) in the nonpigmented ciliary epithelium. Perls' label was also detected in the RPE of the 7-month-old DKO.

Levels of L-Ferritin in DKO Ciliary Bodies

The levels of ferritin light chain (L-ferritin) are controlled by intracellular iron levels through the iron regulatory protein.²³ To determine whether L-ferritin levels are altered in the ciliary body of the DKO, we immunolabeled the retina and ciliary body with anti-L-ferritin. Levels of L-ferritin increased in the nonpigmented ciliary epithelium of 7-month-old DKO mice in comparison to those in age-matched wild-type or single knockout *Cp* or *Heph* mice (Figs. 1C-F).

Levels of Transferrin Receptor in DKO Retinas

Transferrin receptor mediates cellular iron uptake. Like ferritin, its levels are controlled by the iron regulatory proteins in response to cellular iron levels and move in the opposite direction from ferritin levels; in response to increased iron, TfR levels decrease. To test whether the DKO retinas have altered TfR levels, we immunolabeled 7-month-old DKO and age-matched wild-type retinas with anti-TfR. As expected in iron-overloaded tissue, TfR, while present in all retinal cell layers in the wild-type, was undetectable in the DKO, except for a thin layer near the junction of photoreceptor inner and outer segments (Fig. 2).

Iron Quantification by Atomic Absorption in the Retinas and RPE/Choroid of DKO and Wild-Type Eyes with Age

Neurosensory retinas (without RPE) of 6-month-old DKO mice ($n = 6$) had significantly higher iron levels in comparison with age-matched wild-type (Fig. 3A; $n = 4$). Also, iron levels were significantly higher in 6-month-old DKO neurosensory retinas than in 3-month-old DKO ($n = 6$). Iron accumulation in the DKO retinas reached a plateau at 6 months, and there was a slight, nonsignificant increase at 9 months. At 6 months, the iron levels were increased in the DKO relative to wild-type by approximately 2.5-fold.

In RPE/choroid samples (Fig. 3B), a significant difference in iron levels was found among the following groups: 3-month-old DKO ($n = 6$) versus wild-type ($n = 6$) mice, and 6-month-old DKO ($n = 6$) versus wild-type ($n = 4$) mice, as well as 3- versus 6-month-old DKOs. As in the retinas, it was apparent that the iron levels in the RPE/choroid samples plateaued at ~6 months of age, as the slight increase in iron between 6 and 9 ($n = 4$) months in DKO mice was not significant. At 6 months, iron levels increased by approximately 4.5-fold in the DKO relative to wild-type.

Isoprostane F2 α -VI Levels in DKO Mice in Comparison to Age-Matched Wild-Type

Isoprostane F2 α -VI is a product of nonenzymatic oxidation of polyunsaturated fatty acids by reactive oxygen species. It serves as a quantitative, specific marker of oxidative stress in the retina.¹⁸ The levels were significantly increased (Fig. 3C) in 6-month-old DKO retinas ($n = 4$) in comparison with 6-month-old wild-type ($n = 10$).

Age-Dependent Retinal Degeneration with Neovascularization in DKO Mice

Retinas from DKOs younger than 6 months appeared normal. In comparison with wild-type (Fig. 4A), 7-month-old DKO mice had focal areas of retinal degeneration generally involving less than 10% of the retina. The degeneration consisted of RPE hyperplasia (Fig. 4B), RPE hypertrophy, and focal photoreceptor degeneration characterized by thinning of the ONL, inner segment vacuolization, and loss of outer segments. Sparse macrophages were present between the RPE and outer segments (Fig. 4C). In DKO mice at the age of 9 months, the retinal degeneration was generally more severe than at 7 months. There were focal areas of hypertrophic RPE cells with loss of overlying photoreceptor outer segments and thinning of the ONL (Fig. 4D). Hypertrophic RPE cells were found in as much as a quarter of the retinal length. Nine-month-old DKOs also tended to have more macrophage infiltration than at 7 months of age (Fig. 4E). In 12- to 13-month-old DKOs, the degeneration was more severe. Hypertrophic RPE cells were evident in 90% of the total retinal length, along with loss of inner and outer segments, thinning of the ONL (Fig. 4F), and subretinal macrophage infiltration. Focal areas of neovascularization occurred in three-fourths of the 12- to 13-month-old mice and approximately half of mice ranging from 7- to 9 months old. The neovascularization was detected by using cardiac perfusion with DiI followed by epifluorescence microscopy of the eyecups. While wild-types had no neovascularization (Fig. 4G), DKOs had focal areas of hyperfluorescence (Fig. 4H). These areas corresponded on histologic sections to focal RPE disruption with vessels extending from the basal side of the RPE through the photoreceptor layer (Fig. 4I).

Subretinal Macrophage Infiltration in DKO Mice

The frequency and distribution of macrophage infiltrates and their association with neovascularization, atrophy of the retinal pigment epithelium, and the breakdown of Bruch's membrane suggest that AMD has a chronic inflammatory component.²⁴ Macrophages have also been associated with phagocytosis of wide-spaced collagen, which may be a stimulus for inflammation.²⁵ Although the age-matched wild-type mouse retinas had no macrophage infiltration (data not shown), 9- and 13-month-old DKOs had sparse macrophage infiltration present between the RPE and outer segments (Fig. 5).

Accumulation of Lipofuscin-like Material in the DKO RPE with Age

Lipofuscin accumulation has been described in the aging human eye and in AMD. Although the aged-matched wild-type mouse retinas had no detectable autofluorescent lipofuscin in the RPE (Fig. 6A, 6C), DKOs had RPE autofluorescence. Focal areas of autofluorescent hypertrophic RPE were present in 7- to 9-month-old DKO retinas (Figs. 6B, 6D), and most of the RPE cells in the 12-month-old DKO were autofluorescent (Fig. 6E). Like human RPE lipofuscin, the spectrum of autofluorescence was broad, including emission in the green spectrum (excitation = 460–500 nm, barrier filter = 510–560 nm) when excited with blue light (Figs. 6B, 6E) and emission in the red spectrum (Fig. 6D; excitation = 530–560 nm, barrier filter = 573–648 nm) when excited with green light.

Activated Complement Components in DKO Bruch's Membrane

The complement cascade has been implicated in the pathogenesis of AMD by histologic and genetic studies.^{26–30} Activated complement components have been detected in drusen from human donor AMD retinas. To determine whether the pathogenesis of

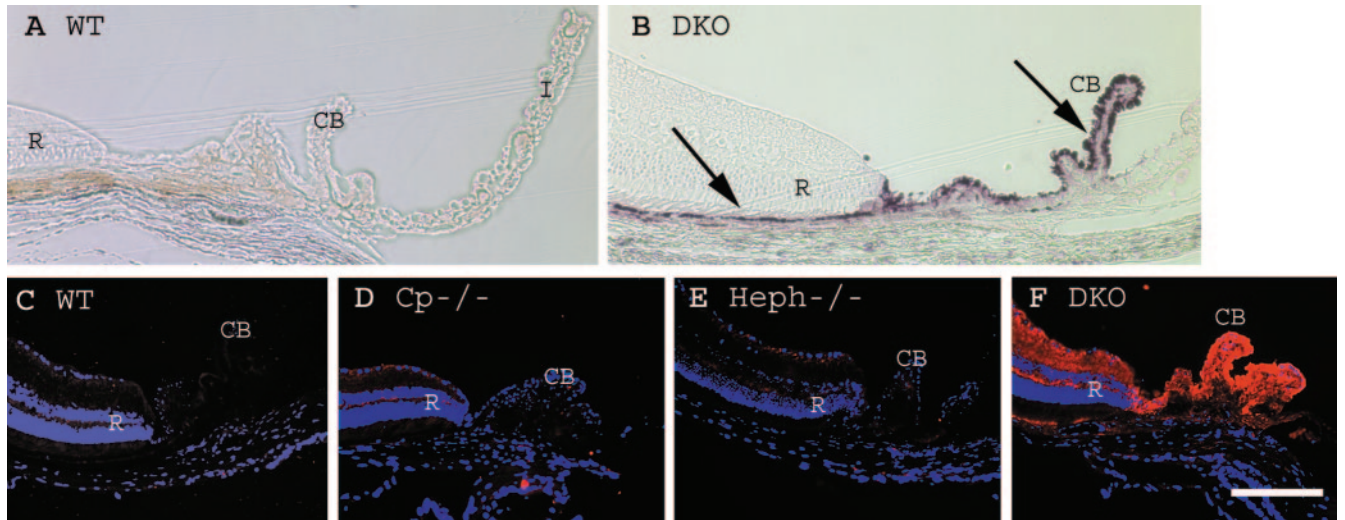


FIGURE 1. The $Cp^{-/-}Heph^{-/-}$ (DKO) ciliary body had iron accumulation and increased L-ferritin. WT (A) and DKO (B) ciliary body Perls' stained (purple) for iron. The 7-month-old DKO ciliary body had detectable iron but the 16-month-old WT control did not. Arrows: Perls' label in the nonpigmented ciliary epithelium and in the RPE. Fluorescence photomicrographs of WT (C), $Cp^{-/-}$ (D), $Heph^{-/-}$ (E), and DKO (F) ciliary bodies immunolabeled for L-ferritin (red), counter-stained with DAPI (blue) and imaged with identical exposure parameters. Scale bar: 50 μ m. CB, ciliary body; I, iris; R, retina.

retinal degeneration in the DKO mice may involve complement activation, we immunolabeled DKO retinas with anti-C3b/iC3b/C3c, which is specific for activated complement. While age-matched wild-type retinas had no detectable label (Fig. 7A), 9-month-old DKOs had sub-RPE label within Bruch's membrane in focal stretches (Fig. 7B), each as long as 200 μ m.

DISCUSSION

In wild-type mice, both ferroxidases Cp and Heph are present in RPE and neurosensory retina,⁸ where they are believed to facilitate iron export from the cells by oxidizing ferrous to ferric iron, the only form that can be taken up by the transport

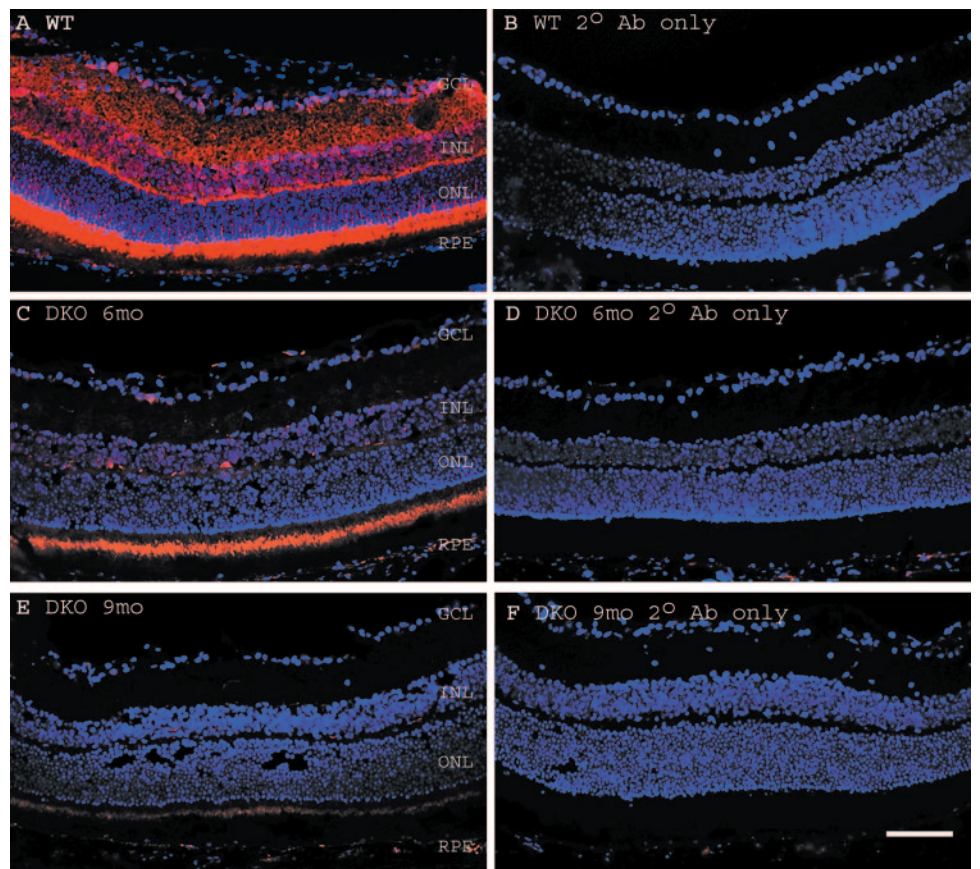


FIGURE 2. Levels of TfR decreased in DKO retinas. Fluorescence photomicrographs of WT retina (A) immunolabeled with anti-TfR antibodies (red), showed strong immunoreactivity present in all retinal cell layers. In contrast, except for a thin line of immunoreactivity near the junction of the photoreceptor inner and outer segments, immunoreactivity in the remainder of the retina was weak in the 6-month-old DKO (C) and was minimal in the 9-month-old DKO (E) mice. (B, D, F) Matching controls for WT and 6- and 9-month-old DKO mice without primary antibodies. Identical exposure parameters were used. RPE, retinal pigment epithelium; ONL, outer nuclear layer; INL, inner nuclear layer; GCL, ganglion cell layer. Scale bar, 50 μ m.

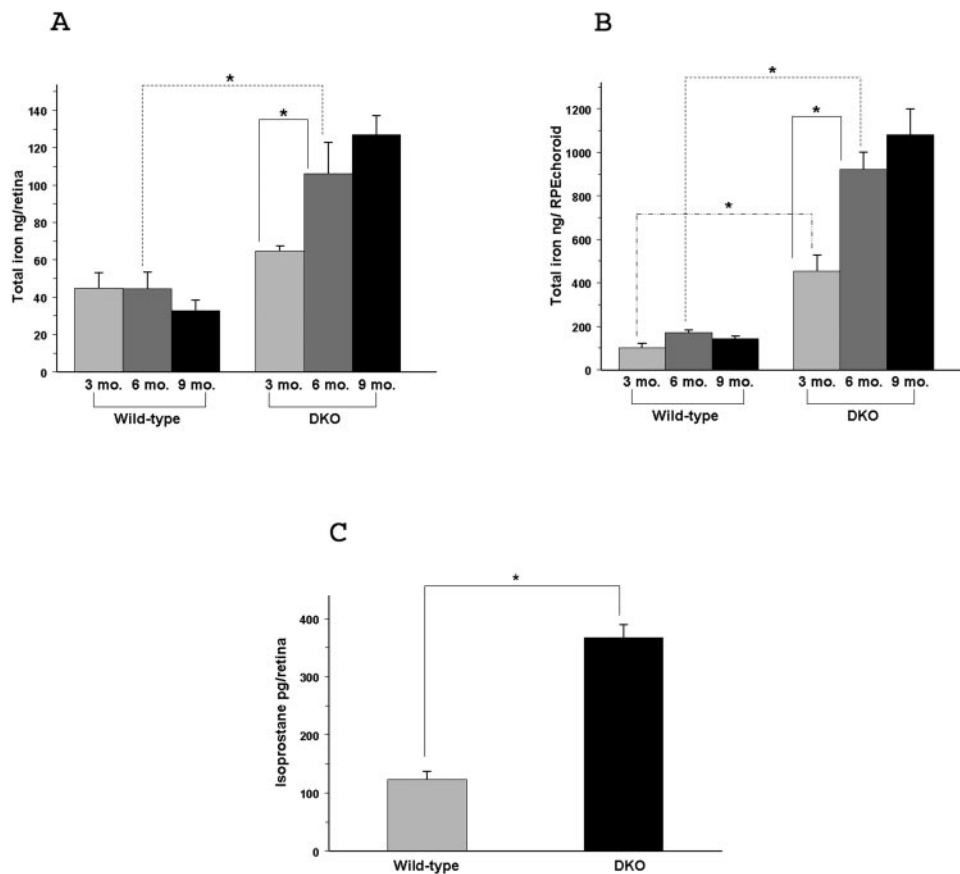


FIGURE 3. Graphs of iron and isoprostane quantification in the retinas and RPE/choroid of DKO and wild-type eyes with age. Total iron in nanograms per neurosensory retina (A) measured by atomic-absorption spectrometry (AAS) is shown for age and genotype. Total iron in nanograms per RPE/choroid measured by AAS (B) is shown for age and genotype. Isoprostane F2 α -VI levels (C) measured by mass spectrometry are shown for 6-month-old DKO in comparison to 6-month-old wild-type neurosensory retinas. *Significant difference ($P < 0.05$).

protein transferrin. Mice deficient in both ferroxidases (DKOs) developed age-dependent retinal iron overload and ultimately retinal degeneration. Elevations in iron levels in DKO retinas resulted in increased levels of the cytosolic iron storage protein ferritin.⁸

In this study, increased L-ferritin was observed in the DKO ciliary body, which was consistent with elevated iron levels in this location detected by Perls' stain. The functions of the ciliary body include secretion of aqueous humor, glycoproteins of the vitreous body, antioxidant enzymes, and neuropeptides.³¹ The aqueous humor is almost completely isolated from the blood in the ciliary body stroma by an epithelium.³² The ciliary body is composed of two polarized neuroepithelial cell layers: pigmented and nonpigmented. Tight junctions in the ciliary epithelium are restricted to the apical plasma membrane of the nonpigmented cell layer establishing a functional blood-aqueous barrier.³³ Several studies revealed that the ciliary body expresses transferrin³⁴ and ceruloplasmin.³² It has been suggested that these two metalloproteins could act synergistically to decrease formation of reactive oxygen intermediates (ROIs) in the aqueous and vitreous, which are in close contact with the retina, lens, trabecular meshwork, and cornea.³² The reason for iron accumulation in the nonpigmented epithelial layer in the DKOs is unclear, but suggests that iron normally passes through this layer, and the transit is dependent on Cp and Heph. It is possible that iron is normally transported by the nonpigmented epithelium into the aqueous, where it would bind transferrin and supply the iron needs of the nonvascularized ocular tissues: the lens epithelium and the cornea. In support of this hypothesis, there is strong immunoreactivity to TfR antibodies in the human lens epithelium³⁵ and corneal endothelium.³⁶

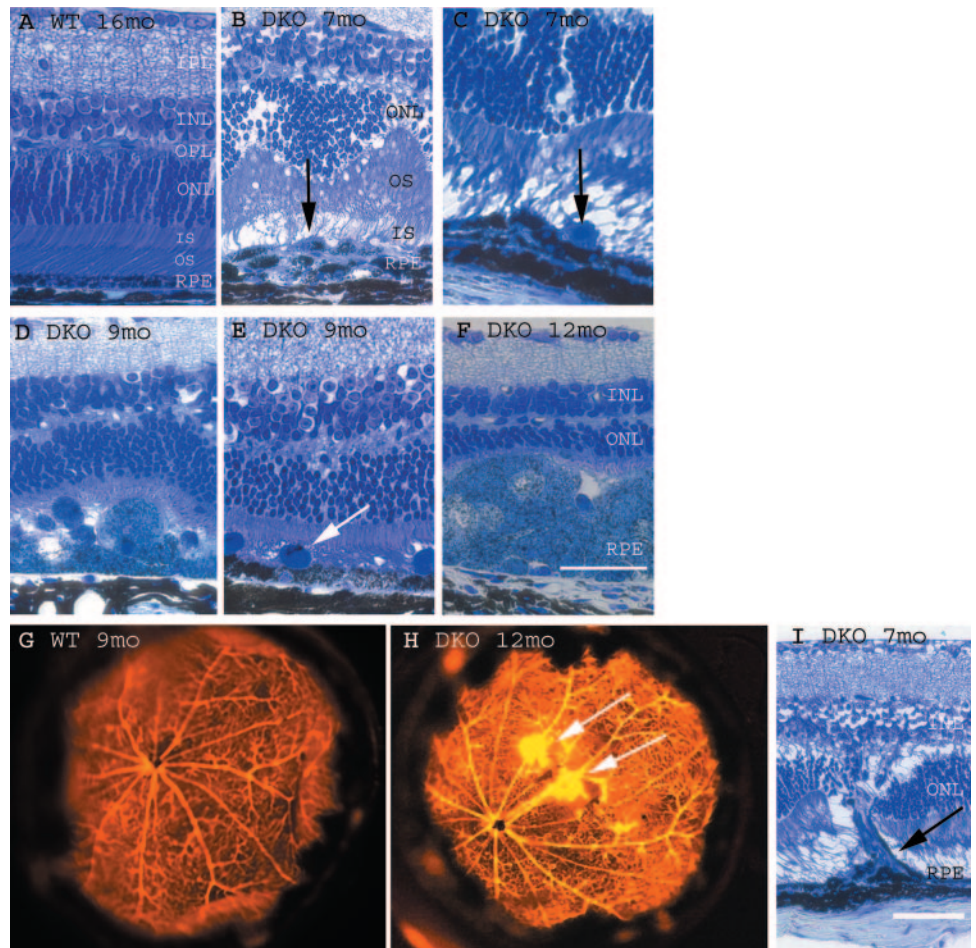
The iron-overloaded DKO retinas had a decrease in levels of TfR. Intracellular iron concentrations are regulated by two iron

regulatory proteins: IRP1 and -2. When cytoplasmic iron is low, IRPs bind to the iron regulatory element (IRE) in the 3'-untranslated region of the TfR's mRNA, stabilizing the mRNA. Conversely, when iron levels are high, the IRP binds iron and dissociates from the TfR's mRNA, leading to degradation of the mRNA and decreased TfR protein levels. Thus, the decreased levels of TfR in DKO retinas most likely represent an appropriate regulatory response to iron overload, preventing further iron uptake in iron-overloaded retinas.

Mice deficient in Cp and Heph showed age-dependant retinal iron accumulation followed by degeneration. This degeneration shared many features with AMD, including RPE hypertrophy and hyperplasia, photoreceptor degeneration, RPE lipofuscin accumulation, subretinal neovascularization, and sub-RPE deposits. These deposits have been observed at the electron microscopic level,⁸ but are not large enough to be detected at the light microscopic level (unlike the drusen and basal linear deposits seen in AMD eyes) representing a difference between human AMD and the DKO mice. Perhaps larger deposits will develop in conditional Cp/Heph-knockout mice, which should live a full lifespan.

The retinal degeneration in the DKO mice was first evident at 6 months of age, and progressed at a variable rate. Mice that survived until 12 to 13 months all had RPE hypertrophy involving 90% of the retina, and most (75%) had subretinal neovascularization. Sparse macrophage infiltration was seen in 90% of 6- to 9-month-old DKOs, and neovascularization was often associated with macrophages, suggesting that the macrophages may promote the neovascularization.³⁷ New blood vessels most likely originated in the choroidal vasculature, as image analysis from thin plastic sections suggested connections between the choroid and the neovascularization. No direct connections between the retinal vasculature and the neovascularization were found, although some sections in

FIGURE 4. DKO mice had age-dependent retinal degeneration with neovascularization. Bright-field micrographs of plastic sections show that relative to 16-month-old WT mice (A) 7-month-old DKO mice had focal areas of RPE hyperplasia (B, *arrow*) and focal photoreceptor degeneration consisting of thinning of the outer nuclear layer (ONL), inner segment vacuolization, and loss of outer segments. Macrophage infiltration was also present (C, *arrow*) in 7-month-old DKO. DKO mice at the age of 9 months (D, E) had focal areas of significantly hypertrophic RPE cells with loss of overlying photoreceptor outer segments and thinning of the ONL. Nine-month-old DKOs had more macrophage infiltration than did the 7-month-old DKOs (E, *arrow*). Twelve-month-old DKOs (F) had hypertrophic RPE cells, loss of inner and outer segments, and thinning of the ONL. Epifluorescence microscopy of eyecups from DiI-perfused mice show that 9-month-old wild-type mice had no neovascularization (G), whereas age-matched DKO (H) had focal areas of hyperfluorescence (*arrows*). These areas correspond to focal RPE disruption, with a vessel passing through the photoreceptor layer, as seen in a 7-month-old DKO retina (I, *arrow*). RPE, retinal pigment epithelium; OS, photoreceptor outer segment; IS, photoreceptor inner segment; ONL, outer nuclear layer; OPL, outer plexiform layer; INL, inner nuclear layer; IPL, inner plexiform layer. Scale bar, 50 μ m.



which NV extended up through the ONL suggest this may occur. Qualitatively, the morphologic changes within each age group were similar, but some variability in the rate and extent of degeneration was found. This variability may be due to exogenous factors such as iron in the diet or maternal genotype, but further investigation will provide insight into the factors influencing these differences.

Quantification of retinal iron by atomic absorption disclosed the location and rate of retina iron build-up in DKOs. Neurosensory retinas of 6-month-old DKOs had significantly higher iron levels in comparison to 3-month-old DKO, but 9-month-old DKOs did not have further significant increase in

iron accumulation. The RPE/choroid had the same trend in iron level increase among the age groups, but iron accumulation was faster and more abundant in comparison with the neurosensory retina. This increase could be either due to the primary function of Cp and Hepb in the RPE or may simply reflect the higher iron flux across the RPE under normal conditions. The lack of further iron accumulation in the retina in 9-month-old DKOs suggests activation of compensatory mechanisms such as the decrease of TfR expression, consistent with Figure 2. Continued retinal degeneration from 9 to 12 months occurs without further iron accumulation, suggesting that it results from cumulative damage from high iron levels already

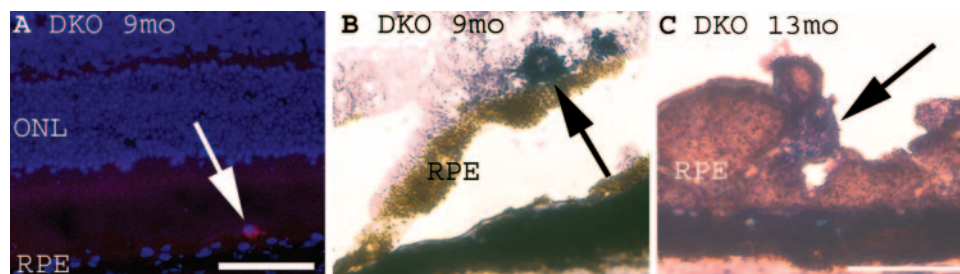


FIGURE 5. Macrophage infiltration in DKO retinas. Fluorescence photomicrograph of 9-month-old DKO (A) immunolabeled with an anti-F4/80 antibody shows subretinal immunoreactivity (*arrow*, red fluorescence) specific for this glycoprotein expressed by macrophages. Bright-field photomicrographs of 9- and 13-month-old DKO retinas (B, C) labeled with anti-CD11b antibodies show Mac-1-positive cells (*arrows*, blue chromogen) specific for macrophages. RPE, retinal pigment epithelium; ONL, outer nuclear layer. Scale bar: (A) 50 μ m; (B, C) 25 μ m.

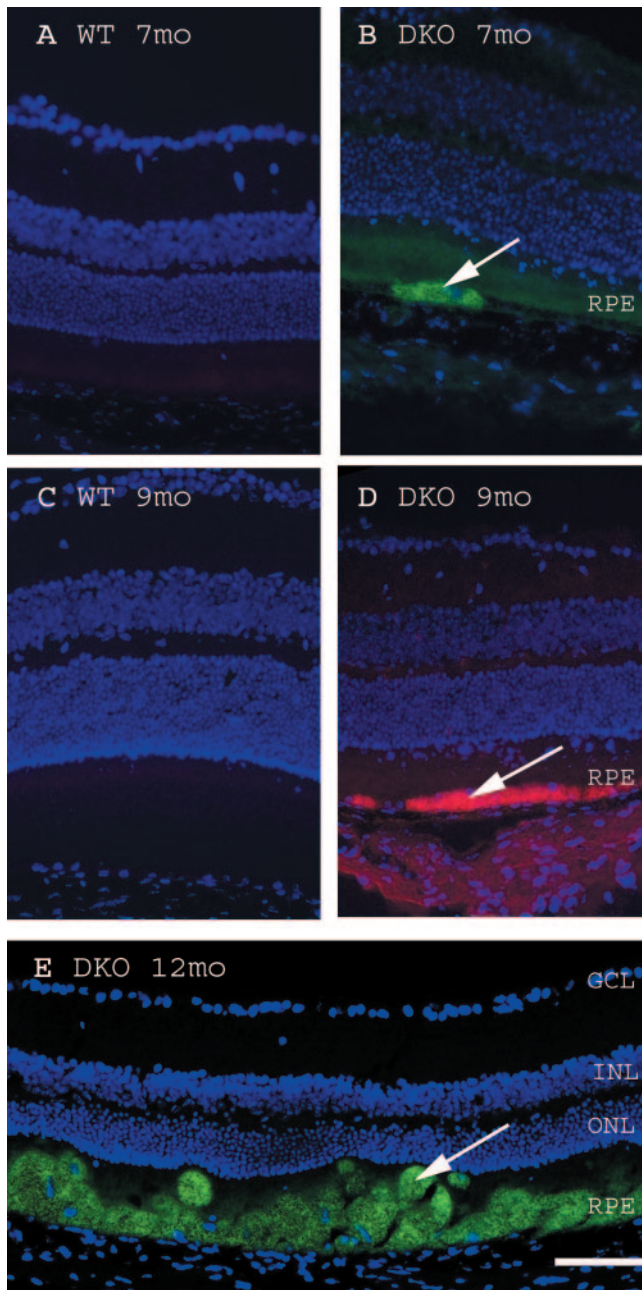


FIGURE 6. Lipofuscin accumulated in the DKO RPE with age. Whereas the aged-matched wild-type retinas had no detectable autofluorescent lipofuscin in the RPE (A, C), DKOs had RPE autofluorescence (B, D, E, arrows). Focal areas of autofluorescent hypertrophic RPE were present in 7-month-old (B, arrow) and 9-month-old (D, arrow) DKO retinas. In 12-month DKOs (E, arrow) most of the RPE cells were autofluorescent. RPE, retinal pigment epithelium; ONL, outer nuclear layer; INL, inner nuclear layer; GCL, ganglion cell layer. Scale bar, 50 μ m.

present at 6 months. This continued retinal degeneration in DKOs older than 9 months may be coming from iron-facilitated oxidative stress. The highly reproducible rate of iron accumulation in DKOs measured by atomic absorption should facilitate further investigations of iron chelators.

Since iron can mediate the generation of free radicals via the Fenton reaction, iron-overloaded retinas from DKO mice are likely to experience a higher amount of oxidative stress. Because isoprostane has been found to be a reliable measure of

oxidative stress,³⁸ this indicator was used in the present study. Results showed negative correlation between Cp and Heph expression and isoprostane levels, suggesting that iron mediated oxidative stress is likely to contribute to the retinal degeneration.

With aging, the autofluorescent pigment lipofuscin accumulates in the cytoplasm of many cell types³⁹ including the RPE. Lipofuscin is not just a harmless hallmark of aging, since lipofuscin-loaded cells have decreased capacity to phagocytose rod outer segments,⁴⁰ and have increased susceptibility to light toxicity.⁴¹ One component of lipofuscin, the bis-retinoid pigment A2E may promote retinal degeneration.⁴² In this study, we found that autofluorescent lipofuscin-like material accumulates in RPE of DKO mice with age, implying that retinal degeneration in our model may also be promoted or exacerbated by age-related pigment accumulation. The components of lipofuscin can vary from tissue to tissue and within a specific cell type over time, and so there is no strict definition of lipofuscin. The autofluorescence in the DKO RPE meets several of the criteria generally associated with lipofuscin: It has a broad spectrum; is bleached by 5 mM CuSO_4 but not H_2O_2 , KMnO_4 , KMnO_4 plus oxalic acid, or NaBH_4 (data not shown)⁴³; and observed in hypertrophic RPE cells, the cytoplasm of which is packed with lysosomes/endosomes.⁸ Studies on the biochemical composition of the lipofuscin within the DKO RPE must await generation of additional 12-month-old DKOs. Since they rarely live to this age, RPE-specific conditional knockouts, which have normal viability, would facilitate this analysis.

An increasing number of studies propose local inflammation and activation of the complement cascade in the pathogenesis of AMD. The complement system plays an important role in a variety of disease processes. Under normal conditions local complement activation is protective against pathogens. Uncontrolled activation of complement can damage host cells and tissues and contribute to disease progression. It has been suggested that photooxidation of RPE lipofuscin continues over time and contributes to inflammation in AMD. Photooxidation products then could be recognized by the complement system which would lead to its activation and to low-grade inflammation.⁴² Also, it has been suggested that drusen form or enlarge

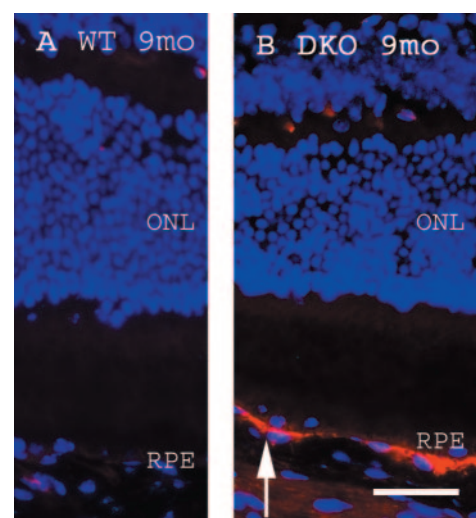


FIGURE 7. Activated complement components were present in DKO Bruch's membrane. Fluorescence photomicrograph of 9-month-old WT immunolabeled with anti-C3b/iC3b/C3c antibodies showed no immunoreactivity, whereas there was sub-RPE immunoreactivity (arrow) in a 9-month-old DKO RPE, retinal pigment epithelium. ONL, outer nuclear layer. Scale bar, 50 μ m.

as a product of a local inflammatory processes,^{44,45} as they contain numerous inflammatory proteins.^{29,46} Many of these proteins are associated with complement system activation and regulation. In this study, we found sub-RPE immunoreactivity for activated complement, suggesting that in our model, retinal degeneration may be associated with inflammatory processes. Complement activation has also been observed in other mouse models of AMD caused by various upstream mechanisms including defects in macrophage recruitment⁴⁷ and mutation of fibulin-3, an extracellular matrix component.⁴⁸

Iron is an essential element in human metabolism but also is a very potent generator of oxidative stress. Evidence supports a role of iron overload in AMD. Earlier, we found that iron levels within the human retina increase with age.² Further, it has been shown that relative to age-matched control retinas, retinas of patients with AMD have elevated iron levels that may contribute to retinal degeneration.⁸ Patients with hereditary diseases causing retinal iron overload such as aceruloplasminemia, Friedreich's ataxia, and pantothenate kinase-associated neurodegeneration, have retinal degeneration.¹ Our DKO mice had iron overload and features of AMD, making them a model for this disease, and also a good model of iron chelation or antioxidant therapy. The presence of lipofuscin and complement activation in both AMD and the DKOs increases the likelihood that the DKOs model some mechanistic features of AMD. Future development of conditional Hepb knockout mice should facilitate these studies, both by providing information about the cell-autonomous function of Hepb, and by providing a more abundant supply of mice, which unlike the current DKOs, will be fertile and have a normal lifespan.

Acknowledgments

The authors thank Chih King for histology.

References

- Dunaief JL. Iron induced oxidative damage as a potential factor in age-related macular degeneration: the Cogan Lecture. *Invest Ophthalmol Vis Sci.* 2006;47:4660-4664.
- Hahn P, Ying GS, Beard J, Dunaief JL. Iron levels in human retina: sex difference and increase with age. *Neuroreport.* 2006;17:1803-1806.
- Dallman PR, Siimes MA, Stekel A. Iron deficiency in infancy and childhood. *Am J Clin Nutr.* 1980;33:86-118.
- Hentze MW, Muckenthaler MU, Andrews NC. Balancing acts: molecular control of mammalian iron metabolism. *Cell.* 2004;117:285-297.
- Rouault T, Klausner R. Regulation of iron metabolism in eukaryotes. *Curr Top Cell Regul.* 1997;35:1-19.
- Williams DM, Lee GR, Cartwright GE. Ferritinase activity of rat ceruloplasmin. *Am J Physiol.* 1974;227:1094-1097.
- Jeong SY, David S. Glycosylphosphatidylinositol-anchored ceruloplasmin is required for iron efflux from cells in the central nervous system. *J Biol Chem.* 2003;278:27144-27148.
- Hahn P, Qian Y, Dentchev T, et al. Disruption of ceruloplasmin and hephaestin in mice causes retinal iron overload and retinal degeneration with features of age-related macular degeneration. *Proc Natl Acad Sci U S A.* 2004;101:13850-13855.
- Vulpe CD, Kuo YM, Murphy TL, et al. Hephaestin, a ceruloplasmin homologue implicated in intestinal iron transport, is defective in the sla mouse. *Nat Genet.* 1999;21:195-199.
- Hahn P, Beard J, Dunaief J. Increased retinal iron levels with age. *Neuroreport.* 2006;17(17):1803-1806.
- Gitlin JD. Aceruloplasminemia. *Pediatr Res.* 1998;44:271-276.
- Miyajima H, Kono S, Takahashi Y, Sugimoto M. Increased lipid peroxidation and mitochondrial dysfunction in aceruloplasminemia brains. *Blood Cells Mol Dis.* 2002;29:433-438.
- Dunaief JL, Richa C, Franks EP, et al. Macular degeneration in a patient with aceruloplasminemia, a disease associated with retinal iron overload. *Ophthalmology.* 2005;112:1062-1065.
- Hahn P, Milam AH, Dunaief JL. Maculas affected by age-related macular degeneration contain increased chelatable iron in the retinal pigment epithelium and Bruch's membrane. *Arch Ophthalmol.* 2003;121:1099-1105.
- Klein R, Wang Q, Klein BE, Moss SE, Meuer SM. The relationship of age-related maculopathy, cataract, and glaucoma to visual acuity. *Invest Ophthalmol Vis Sci.* 1995;36:182-191.
- Perry G, Sayre LM, Atwood CS, et al. The role of iron and copper in the aetiology of neurodegenerative disorders: therapeutic implications. *CNS Drugs.* 2002;16:339-352.
- Erikson KM, Pinero DJ, Connor JR, Beard JL. Regional brain iron, ferritin and transferrin concentrations during iron deficiency and iron repletion in developing rats. *J Nutr.* 1997;127:2030-2038.
- Dentchev T, Yao Y, Pratico D, Dunaief J. Isoprostane F2alpha-VI, a new marker of oxidative stress, increases following light damage to the mouse retina. *Mol Vis.* 2007;13:190-195.
- Pratico D, Lee VM-Y, Trojanowski JQ, Rokach J, Fitzgerald GA. Increased F2-isoprostanes in Alzheimer's disease: evidence for enhanced lipid peroxidation in vivo. *FASEB J.* 1998;12:1777-1783.
- Pratico D, Clark CM, Lee VM, Trojanowski JQ, Rokach J, Fitzgerald GA. Increased 8,12-iso-iPF2alpha-VI in Alzheimer's disease: correlation of a noninvasive index of lipid peroxidation with disease severity. *Ann Neurol.* 2000;48:809-812.
- Dunaief JL, Dentchev T, Ying G-S, Milam AH. The role of apoptosis in age-related macular degeneration. *Arch Ophthalmol.* 2002;120:1435-1442.
- Zhao L, Wang Z, Liu Y, et al. Translocation of the retinal pigment epithelium and formation of sub-retinal pigment epithelium deposit induced by subretinal deposit. *Mol Vis.* 2007;13:873-880.
- Haile DJ, Rouault TA, Tang CK, Chin J, Harford JB, Klausner RD. Reciprocal control of RNA-binding and aconitase activity in the regulation of the iron-responsive element binding protein: role of the iron-sulfur cluster. *Proc Natl Acad Sci USA.* 1992;89:7536-7540.
- Penfold P, Killingsworth M, Sarks S. An ultrastructural study of the role of leucocytes and fibroblasts in the breakdown of Bruch's membrane. *Aust J Ophthalmol.* 1984;12:23-31.
- Penfold PL, Killingsworth MC, Sarks SH. Senile macular degeneration: the involvement of immunocompetent cells. *Graefes Arch Clin Exp Ophthalmol.* 1985;23:69-76.
- Klein RJ, Zeiss C, Chew EY, et al. Complement factor H polymorphism in age-related macular degeneration. *Science.* 2005;308:385-389.
- Edwards AO, Ritter R 3rd, Abel KJ, Manning A, Panhuysen C, Farrer LA. Complement factor H polymorphism and age-related macular degeneration. *Science.* 2005;308:421-424.
- Hageman GS, Anderson DH, Johnson LV, et al. A common haplotype in the complement regulatory gene factor H (HF1/CFH) predisposes individuals to age-related macular degeneration. *Proc Natl Acad Sci USA.* 2005;102:7227-7232.
- Johnson LV, Ozaki S, Staples MK, Erickson PA, Anderson DH. A potential role for immune complex pathogenesis in drusen formation. *Exp Eye Res.* 2000;70:441-449.
- Nozaki M, Raisler BJ, Sakurai E, et al. Drusen complement components C3a and C5a promote choroidal neovascularization. *Proc Natl Acad Sci USA.* 2006;103:2328-2333.
- Coca-Prados M, Escibano J, Ortego J. Differential gene expression in the human ciliary epithelium. *Prog Retin Eye Res.* 1999;18:403-429.
- Bertazzoli-Filho R, Laicine EM, Haddad A, Rodrigues ML. Molecular and biochemical analysis of ceruloplasmin expression in rabbit and rat ciliary body. *Curr Eye Res.* 2006;31:155-161.
- Coca-Prados M, Escibano J. New perspectives in aqueous humor secretion and in glaucoma: the ciliary body as a multifunctional neuroendocrine gland. *Prog Retin Eye Res.* 2007;26:239-262.
- Bertazzoli-Filho R, Laicine EM, Haddad A. Synthesis and secretion of transferrin by isolated ciliary epithelium of rabbit. *Biochem Biophys Res Commun.* 2003;305:820-825.
- Baudouin C, Brignole F, Fredj-Reygrobelle D, Negre F, Bayle J, Gastaud P. Transferrin receptor expression by retinal pigment epithelial cells in proliferative vitreoretinopathy. *Invest Ophthalmol Vis Sci.* 1992;33:2822-2829.

36. Tan PH, King WJ, Chen D, et al. Transferrin receptor-mediated gene transfer to the corneal endothelium. *Transplantation*. 2001;71:552-560.
37. Shen J, Xie B, Dong A, Swaim M, Hackett SF, Campochiaro PA. In vivo immunostaining demonstrates macrophages associate with growing and regressing vessels. *Invest Ophthalmol Vis Sci*. 2007;48:4335-4341.
38. Pratico D. F(2)-isoprostanes: sensitive and specific non-invasive indices of lipid peroxidation in vivo. *Atherosclerosis*. 1999;147:1-10.
39. Brizzee KR, Ordy JM, Kaack B. Early appearance and regional differences in intraneuronal and extraneuronal lipofuscin accumulation with age in the brain of a nonhuman primate (*Macaca mulatta*). *J Gerontol*. 1974;29:366-381.
40. Sundelin S, Wihlmark U, Nilsson SE, Brunk UT. Lipofuscin accumulation in cultured retinal pigment epithelial cells reduces their phagocytic capacity. *Curr Eye Res*. 1998;17:851-857.
41. Wihlmark U, Wrigstad A, Roberg K, Nilsson SE, Brunk UT. Lipofuscin accumulation in cultured retinal pigment epithelial cells causes enhanced sensitivity to blue light irradiation. *Free Radic Biol Med*. 1997;22:1229-1234.
42. Zhou J, Jang YP, Kim SR, Sparrow JR. Complement activation by photooxidation products of A2E, a lipofuscin constituent of the retinal pigment epithelium. *Proc Natl Acad Sci USA*. 2006;103:16182-16187.
43. Schnell SA, Staines WA, Wessendorf MW. Reduction of lipofuscin-like autofluorescence in fluorescently labeled tissue. *J Histochem Cytochem*. 1999;47:719-730.
44. Hageman GS, Luthert PJ, Victor Chong NH, Johnson LV, Anderson DH, Mullins RF. An integrated hypothesis that considers drusen as biomarkers of immune-mediated processes at the RPE-Bruch's membrane interface in aging and age-related macular degeneration. *Prog Retin Eye Res*. 2001;20:705-732.
45. Crabb JW, Miyagi M, Gu X, et al. Drusen proteome analysis: an approach to the etiology of age-related macular degeneration. *Proc Natl Acad Sci USA*. 2002;99:14682-14687.
46. Anderson DH, Mullins RF, Hageman GS, Johnson LV. A role for local inflammation in the formation of drusen in the aging eye. *Am J Ophthalmol*. 2002;134:411-431.
47. Ambati J, Anand A, Fernandez S, et al. An animal model of age-related macular degeneration in senescent Ccl-2- or Ccr-2-deficient mice. *Nat Med*. 2003;9:1390-1397.
48. Fu L, Garland D, Yang Z, et al. The R345W mutation in EFEMP1 is pathogenic and causes AMD-like deposits in mice. *Hum Mol Genet*. 2007;16:3411-3422.